MOMENT-CURVATURE MODEL FOR FLEXURAL ASSESSMENT OF TEXTILE-REINFORCED CONCRETE BEAMS

H. Spartali[1], S. Rastegarian[2], N. Will[3], R. Chudoba[4]

[1] *H. Spartali, Institute of Structural Concrete, RWTH Aachen University, Aachen, Germany, hspartali@imb.rwth-aachen.de*

[2] *S. Rastegarian, Institute of Structural Concrete, RWTH Aachen University, Aachen, Germany, saeed.rastegarian@rwth-aachen.de*

[3] *N. Will, Institute of Structural Concrete, RWTH Aachen University, Aachen, Germany, nwill@imb.rwth-aachen.de*

[4] *R. Chudoba, Institute of Structural Concrete, RWTH Aachen University, Aachen, Germany, rostislav.chudoba@rwth-aachen.de*

SUMMARY: *Several numerical models reflecting the flexural response of steel-reinforced concrete beams have been developed in the past. However, their adaption to carbon-reinforced concrete needs to consider a different type of material behaviour. In addition, they must be able to reflect numerous reinforcement layouts with more flexible configurations of textile fabrics within the cross-section. In this paper, a general cross-section model for the derivation of the moment-curvature and load-deflection curves for concrete beams reinforced with short fibers, bar reinforcement and textile fabrics is introduced, which incorporates materials non-linearities and is easily applicable to cross-sections with arbitrary shapes and reinforcement layouts. The validation shows the ability of the model to reliably reproduce the experimental results.*

KEY WORDS: *textile fabrics, carbon concrete, moment-curvature, SLS, flexural model, nonlinear behaviour, general cross-sections.*

1. INTRODUCTION

A wide range of numerical and analytical models and approaches for the evaluation of the moment-curvature response of steel reinforced concrete elements subjected to bending loading have been presented in the literature [1], [2], [3], [4], [5], [6], [7]. However, most of these models have been established based on specific assumptions for the material models, cross-sectional shape and the layout of the reinforcement layers. Moreover, only few research contributions have handled the case of carbon-reinforced bending elements [8], [9].

Adding to this the fact that, while several concepts for the assessment of the ultimate limit state (ULS) design of carbon-reinforced concrete beams exist, an efficient and flexible approach to the deflection assessment in the serviceability limit state (SLS) is still missing.

In this paper, a generic flexural model for RC bending elements is presented which enables a flexible integration of different material models and an easy selection of any cross-sectional shape and reinforcement layout. This is possible due to the modular implementation of the model code in hierarchal structure of model components using Python programming language in combination with a rapidly evolving ecosystem of scientific computing libraries.

The model can be utilized for different types of concrete composites reinforced with short fibers, bar reinforcement and textile fabrics. It can support the development of hybrid cross-sectional layouts to optimally exploit the properties of high-performance reinforcement materials [10].

The applicability of the model to bending elements is introduced and validated using experimental data on concrete beams reinforced with carbon fabrics, carbon bars and steel bars available in the literature. Using the model, it is possible to generate the moment-curvature curve for a specific configuration of the cross-section for the studied element. Depending on this, the load-deflection response can then be calculated for arbitrary beam support and loading configurations.

The goal of this development is to provide a general, transparent, and efficient assessment procedure for reinforced concrete beam deflection that serves as the basis for applications in engineering practice.

2. MOMENT-CURVATURE MODEL

2.1. General implementation aspects

The computational procedure follows the usual arrangement of the equilibrium and kinematic conditions at a representative cross-section of a beam in combination with non-linear constitutive relations and is similar to the approach described in [10]. For convenience, the kinematic assumption of linear strain profile is directly related to the

cross-sectional curvature κ. In this way, the M-κ relation needed for the deflection evaluation can be efficiently obtained using a set of non-linear equilibrium equations. To achieve maximum flexibility, these equilibrium conditions are formulated and implemented as a general integral function that can incorporate any material law for the reinforcement layers and for the concrete in form of multi-linear or continuous functions. Moreover, arbitrary number of reinforcement layers can be included.

The moment-curvature relationship is obtained by solving the equilibrium of the cross section for a pre-defined relevant range of curvature values. By assuming that the cross-section remains flat after deformation, a linear distribution of normal strains along the cross-sectional height is obtained, which yields

$$\varepsilon(z) = \varepsilon_{\text{bot}} + z \cdot \frac{\varepsilon_{top} - \varepsilon_{\text{bot}}}{h} \quad , \; 0 \leq z \leq h, \tag{1}$$

where ε_{bot} and ε_{top} are the strain values in the bottom and the top of the cross-section, respectively, h is the height of the cross-section and z is the height of the evaluated strain assuming $z = 0$ corresponds to the bottom of the cross-section. The curvature is given as

$$\kappa = -\frac{\mathrm{d}\varepsilon(z)}{\mathrm{d}z} = -\frac{\varepsilon_{\text{top}} - \varepsilon_{\text{bot}}}{h} \Rightarrow \varepsilon_{\text{top}} = -\kappa \cdot h + \varepsilon_{\text{bot}} \tag{2}$$

By combining (1) and (2) we obtain the strain profile over the cross-sectional height

$$\varepsilon(z) = \varepsilon_{\text{bot}} - \kappa \cdot z, \tag{3}$$

where ε_{bot} is unknown. This strain profile is used as an input into the constitutive relations defined for concrete and reinforcement in the next section to obtain the cross-sectional stress profile as a function of $\kappa, z, \varepsilon_{\text{bot}}$.

2.2. Constitutive laws

2.2.1 Constitutive laws for the concrete

Figure 1 shows two types of applicable material laws: type (a) shows a material law, that is used in this paper for model validation and is composed of a piecewise linear function for both the compression and tension regions according to Yao et al. [7].

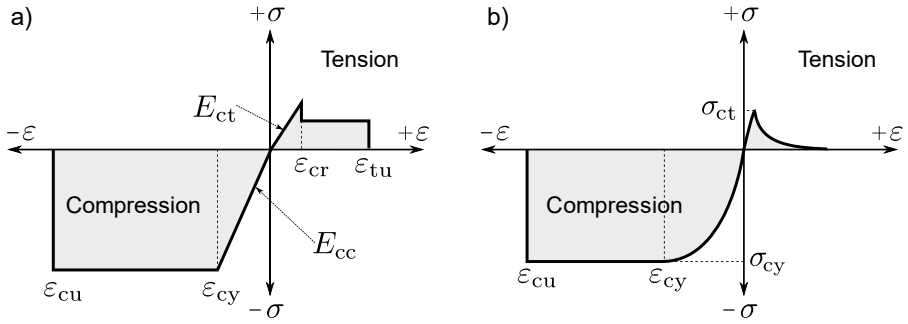

Figure 1. *Two possible variants for the constitutive law for concrete*

The diagram in Figure 1 (b) represents another type of the constitutive law for concrete with a compression curve based on the Eurocode 2 [11] and a continuous curve with nonlinear softening in the tensile regime.

2.2.2 Constitutive laws for the reinforcement

A linear-elastic, brittle model was assumed for the carbon reinforcement as depicted in Figure 2 (a).

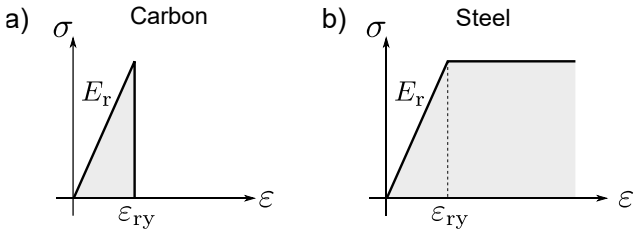

Figure 2. *Constitutive laws used for the reinforcement; a) carbon material law; b) steel material law*

For validation with experimental data with steel reinforcement, the elastic, ideally plastic constitutive law was used for steel , see Figure 2 (b).

The material laws presented above are pre-configured in the model setup. However, the implemented solution algorithm can handle any non-linear material law for both concrete and the reinforcement because the stress values are evaluated for each point along cross-section height.

2.3. Derivation of the moment-curvature relationship

The computational scheme depicted in Figure 3 exemplifies the strain and stress states of a cross-section using the multi-linear concrete constitutive law shown in Figure 1(a). The residual tensile stress in the bottom part of the cross-section represents the

effect of short fibers. The calculation procedure illustrated in Figure 3 is caried out in four steps:

1- The curvature values are assumed in a relevant range of the material behavior with the aim of calculating the corresponding moment values for each given curvature using the equilibrium conditions for normal force and moment in the cross section.

2- By substituting equation (3) into the stress relations of concrete and reinforcement $\sigma_c(\varepsilon)$, $\sigma_r(\varepsilon)$, we obtain the stress distribution over the height z as a function of the given curvature κ and the unknown strain on the cross-section bottom $\varepsilon_{\mathrm{bot}}$. In other words, for each curvature value, we get the stresses in the concrete $\sigma_c(\varepsilon(\kappa, z, \varepsilon_{\mathrm{bot}}))$ and in the reinforcement $\sigma_r(\varepsilon(\kappa, z, \varepsilon_{\mathrm{bot}}))$, according to the used material laws.

3- The stress distribution in the concrete is linearly approximated in a piecewise way along the cross-section height. To determine the concrete contribution of the normal force F_c, the stress at height z is multiplied by the corresponding width $b(z)$ and numerically integrated.

$$F_{\mathrm{c}} = \int_0^h \sigma_c(z) \cdot b(z)\,\mathrm{d}z \tag{4}$$

The normal force from the reinforcement F_r is obtained as the sum of all force contributions in all reinforcement layers, i.e.

$$F_{\mathrm{r}} = \sum_i \sigma_{r_i} \cdot A_{r_i} \tag{5}$$

Assuming that the applied normal force is zero, the equilibrium of normal forces in the cross section is simply given as

$$F_{\mathrm{c}}(\kappa, \varepsilon_{\mathrm{bot}}) + F_{\mathrm{r}}(\kappa, \varepsilon_{\mathrm{bot}}) = 0 \tag{6}$$

4- The cross-section equilibrium is then solved numerically for $\varepsilon_{\mathrm{bot}}$ for each given curvature κ in the relevant range $\kappa \in (0, \kappa_{\mathrm{max}})$. The corresponding bending momentvalue can then be evaluated using the following equation

$$M = \sum F_{\mathrm{r}i} \cdot z_i + \int_z \sigma_{\mathrm{c}} \cdot b \cdot z\,\mathrm{d}z \tag{7}$$

κ_{max} is defined such that the associated moment $M(\kappa_{\mathrm{max}})$ is smaller than that of the maximum reached moment, i.e. beyond the peak of M-κ curve.

The calculation exploits the open-source scientific computing library SciPy allowing an efficient solution of the nonlinear set of equations in parallel on a standard computer.

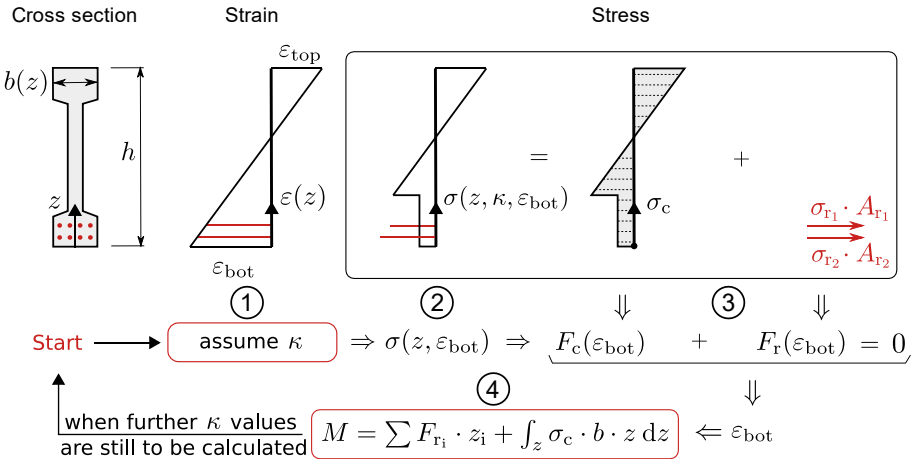

Figure 3. *Summary of the approach used to calculate the moment M corresponding to a given curvature* κ

3. CALCULATION OF THE DEFLECTION

To obtain the beam deflection for an arbitrary configuration of supports and loading, the M-κ curve is inverted into a κ-M curve, as in Figure 4. The moment diagram along the beam is determined for the given loading configuration and discretized as a piecewise linear function along the length of the flexural beam, see Figure 5. At each integration point, the curvature corresponding to the moment is assigned using the M-κ relationship. Finally, the deflection is obtained using a double integration of the curvature curve along the beam over the longitudinal coordinate x, see Figure 5.

The ultimate load for the beam under given boundary conditions F_{max} is calculated using the maximum moment value M_{max} in the M-κ curve, see Figure 4. The relation between the moment and the corresponding force can be obtained from the moment diagram of the beam in its peak value, e.g. for the case of simply supported beam with 4-point bending setup, this can be calculated as $F_{\mathrm{max}} = M_{\mathrm{max}}/x_F$, see Figure 5.

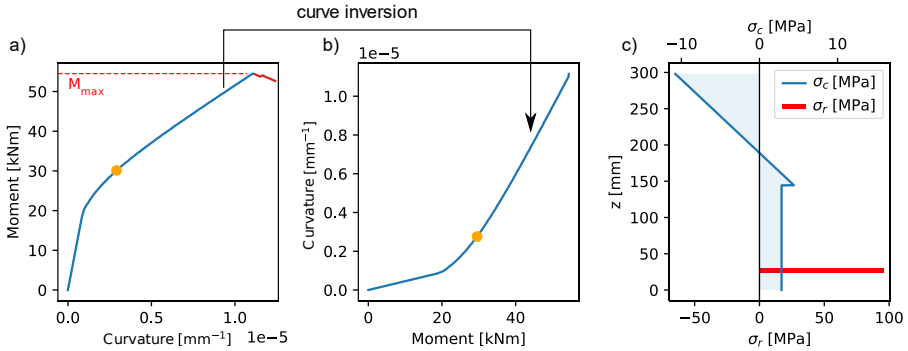

Figure 4. *The calculated M-κ curve with its inversion: a) M-κ curve; b) inverted M-κ curve; c) stress state of the cross-section that corresponds to a loading level indicated by the yellow circle*

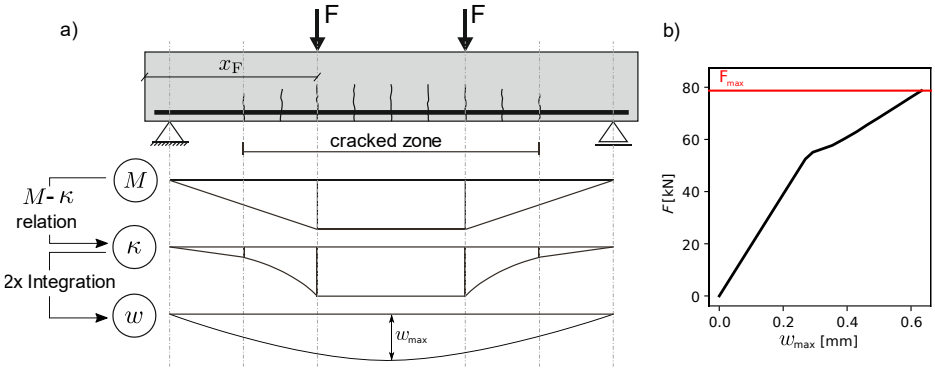

Figure 5. *The calculation of beam deflection based on the obtained M-κ relation.*

4. MODEL VALIDATION WITH EXPERIMENTAL DATA

The moment-curvature and load-deflection curves obtained using the introduced model have been compared with experimental data. To show the feasibility of the model in a broad range of applications, both carbon and steel reinforced concrete sections have been included in the validation. Table 1 summarizes all the used experiments.

Table 1. *List of experiments used for the validation of the model*

	Test ID	ρ [%]	b [mm]	h [mm]	a1 [mm]	a2 [mm]	As1 [mm²]	As2 [mm²]	fs [MPa]	Es [GPa]	fcm [MPa]	Ec [MPa]
Gribniak 2012 (steel)	S3-1-F05	0.3	278	302	24	29	235	56	560	203	56	35000
	S3-1-F15	0.3	279	300	28	26	235	56	560	203	52	34000
Yang 2010 (steel)	R12-1	0.6	180	270	35	-	253	-	600	200	191	46418
	R13-2	0.9	180	270	35	-	380	-	600	200	192	46680
von der Heid 2020* (carbon)	HB-SU-0	0.4	90	30	8	8	7	7	2712	240	72	39500
El Ghadioui 2020 (carbon)	B-M-S-K1	0.6	400	200	19	-	452	-	550	200	64	33525
	B-M-C-K1	0.2	400	200	35	-	140	-	1891	135	64	33525
	B-M-C-K2	0.3	400	200	66	-	140	-	1891	135	64	33525

* Mean values for multiple tests.

4.1. Steel

The first two diagrams in Figure 6 compare the prediction of the M-κ with the experimental results. Figure 6 (a) shows a comparison between M-κ curves for two beams with different short fiber contents conducted by Gribniak et al. [12] and the simulated M-κ response. Two UHPC beams with different reinforcement ratio and a concrete compressive strength $f_{cm} \approx 191$ MPa were conducted by Yang et al. [13]. The experimental M-κ curves are illustrated in Figure 6 (b) with the corresponding curves obtained using the model.

A validation for the load-deflection response for steel reinforcement was provided using experimental results delivered by El Ghadioui et al. [14] for a simply supported beam tested with 4-point bending setup. The load-deflection curves obtained by the model and by the experiment is compared in Figure 6 (c).

The comparison in all three cases shows the ability of the model to correctly reproduce the behavior of the beams including the post-cracking and steel yielding phases of the response.

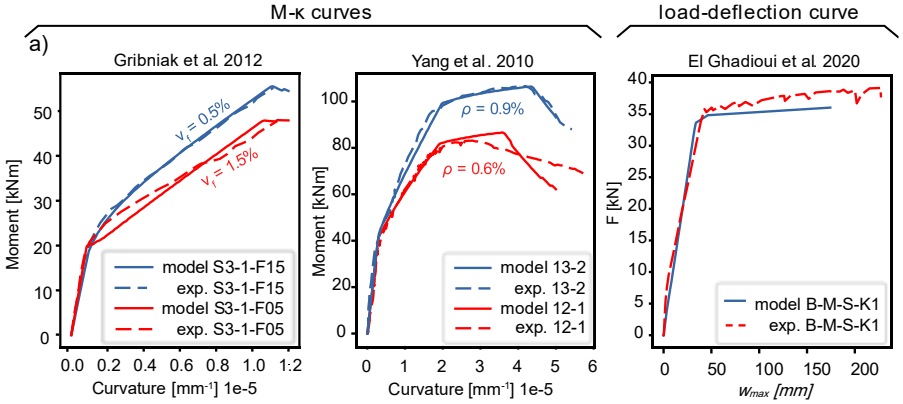

Figure 6: *Comparison between simulated and experimental results for steel-reinforced beams; a),b) M-**κ** curves [12], [13]; c) load-deflection curve [14]*

4.2. Carbon

The load-deflection curves predicted for carbon-reinforced beams by the model are compared with the experimental results in Figure 7.

The experimental results of [14] for two identical beams reinforced with CFRP bars with different static effective heights d are shown in Figure 7 (a). The behavior predicted by the model shows a very good agreement for the initial phase before and after cracking (up to about 10 kN), but after that a slight overestimation of the beam stiffness is observed. This can be attributed to the loss of stiffness due to the multiple cracks, which is evident from the experimental curves and which was not predicted by the current implementation of the model.

The comparison of the test results including two test series by von der Heid et al. [15] with the simulation in terms of the load-deflection curves for the tested plates are shown in Figure 7 (b). The underlying M-κ relation is exemplified in Figure 7 (b*) both for the model and the experiment.

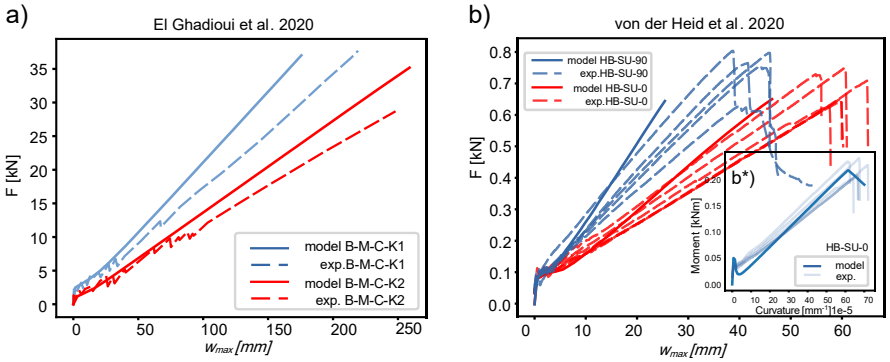

Figure 7: *Comparison between simulated and experimental results for carbon-reinforced elements; a) load-deflection curves by El Ghadioui et al. [14]; b) load-deflection and M-**κ** curves by von der Heid et al. [15]*

5. BASIS FOR SERVICEABILITY DESIGN RULE

The implemented model can serve as a basis of a simple engineering design rule for carbon-reinforced concrete elements in the serviceability limit state (SLS). To comply with the simplified SLS design concept used in the Eurocode 2 [11] and the fib Model Code [16] the relation between the span/depth (L/d) and reinforcement ρ ratios has been evaluated in a parametric study covering the relevant range both for steel and for carbon-reinforced specimens. The results of the study are summarized in Figure 8 showing a qualitatively different shape of the admissible design region. In agreement with the results presented recently by El Ghadioui [17], the carbon reinforced elements exhibit a pronounced transition point between the tensile failure of the reinforcement (left branch) and the compressive failure of concrete (right branch). Two different values of E-moduli and of the carbon tensile strength have been considered in the presented study.

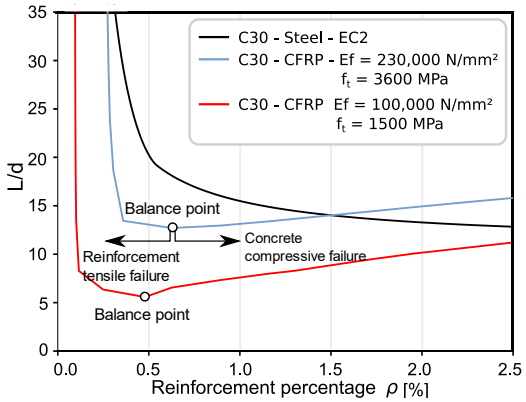

Figure 8: *Comparison between (L/d – ρ) curves for steel and carbon reinforcement*

6. SUMMARY AND CONCLUSION

The described model for the calculation of the moment-curvature relation and the load-deflection response of RC elements exposed to bending load provides a basis for the derivation of general SLS rules as exemplified for beams reinforced with carbon fabrics. The object-oriented model implementation is based on Python programming language and is available on the version control platform GitHub at https://github.com/bmcs-group as part of the brittle-matrix composite structures suite maintained by the authors. This model offers flexibility in several ways. For example, it makes it easy to insert and configure arbitrary types of material models for both concrete and reinforcement, or to use any cross-section shape and reinforcement layout in terms of the number and location of reinforcement layers. The model is based on a numerical piecewise evaluation of the stress and forces along the cross-section and a non-linear solution of the equilibrium of the cross-section that makes use of the SciPy scientific library for Python. The model was validated with experimental data which demonstrated its ability to correctly predict the experimental results for both steel and carbon reinforcement.

In this paper, a multi-linear material law for concrete was used for the validations. In the following refinement steps, more sophisticated constitutive laws will be integrated, exploiting the modular design of the framework. Moreover, an extension of the model to take the effect of the bond behaviour and tension-stiffening in the cracked region along the beam into account is planned. Finally, a comprehensive web application with a wide range of design options will be provided for public access.

7. ACKNOWLEDGMENT

This work was funded by the Deutsche Forschungsgemeinschaft (DFG, German Research Foundation) - SFB/TRR280, Project-ID 417002380.

8. REFERENCES

[1] Pfrang E. O., Siess C. P., and Sozen M., 1964, "Load-Moment-Curvature Characteristics of Reinforced Concrete Cross Sections.", *Journal Proceedings*, 61(7), pp. 763-778.

[2] Domingo J. Carreira, and Kuang-Han Chu, 1986, "The Moment-Curvature Relationship of Reinforced Concrete Members.", *Journal Proceedings*, 83(2), pp. 191-198.

[3] Espion B., and Halleux P., 1988, "Moment curvature relationship of reinforced concrete sections under combined bending and normal force.", *Materials and Structures*, 21(5), pp. 341–351.

[4] W. A. M. Alwis, 1990, "Trilinear Moment-Curvature Relationship for Reinforced Concrete Beams.", *Structural Journal*, 87(3), pp.276-283.

[5] Monti G., and Petrone F., 2015. "Yield and ultimate moment and curvature closed-form equations for reinforced concrete sections.", *ACI Structural Journal* 112(4), p. 463.

[6] Ćurić I., Jure Radic, and Marin Franetovic, 2016. "Determination of the bending moment-curvature relationship for reinforced concrete hollow section bridge columns.", *Tehnicki Vjesnik-Technical Gazette*, 23(3), pp.907-916.
[7] Yao Y., Mobasher B., Wang J., and Xu Q., 2021, "Analytical approach for the design of flexural elements made of reinforced ultra-high performance concrete. ", *Structural Concrete*, 22(1), pp. 298–317.
[8] Barros J. A. O., and Gláucia Dalfré, 2013. "A model for the prediction of the behaviour of continuous RC slabs flexurally strengthened with CFRP systems.", *Proceedings of the 11th International Symposium on Fiber Reinforced Polymers for Reinforced Concrete Structures*, UM, Guimarães.
[9] Rezazadeh M., Barros J., and Costa I., 2015, "Analytical approach for the flexural analysis of RC beams strengthened with prestressed CFRP.", *Composites Part B: Engineering*, 73, pp. 16–34.
[10] Parra-Montesinos, G., and A.E. Naaman, Ed., 2001. "Parametric Evaluation of the Bending Response of Ferrocement and Hybrid Composites with FRP Reinforcements.", *Proceedings of Seventh International Symposium on Ferrocement and Thin Reinforced Cement Composites*, Singapore.
[11] Standardisation E. C. f., 2010, “Eurocode 2: Design of concrete structures - Part 1-1: General rules and rules for buildings. Incl. Corrigendum 1: EN 1992-1-1:2004/AC:2008, incl. Corrigendum 2: EN 1992-1-1:2004/AC:2010,”(EN 1992-1-1:2004).
[12] Gribniak V., Kaklauskas G., Hung Kwan A. K., Bacinskas D., and Ulbinas D., 2012, "Deriving stress–strain relationships for steel fibre concrete in tension from tests of beams with ordinary reinforcement.", *Engineering Structures*, 42, pp. 387–395.
[13] Yang I. H., Joh C., and Kim B.-S., 2010, "Structural behavior of ultra high performance concrete beams subjected to bending.", *Engineering Structures*, 32(11), pp. 3478–3487.
[14] El Ghadioui R., Proske T., Tran N. L., and Graubner C.-A., 2020, "Structural behaviour of CFRP reinforced concrete members under bending and shear loads.", *Materials and Structures*, 53(3), pp.1-16.
[15] Heid A.-C. von der, and Grebe R., 2020, "Perforierte und vollflächige Fassadenplatten aus carbonbewehrtem Beton/Perforated and full-surface façade panels made of carbon-reinforced concrete.", Bauingenieur, 95(06), pp. 210–219.
[16] Beverly P., Ed., 2013. fib model code for concrete structures 2010, Ernst & Sohn, Berlin.
[17] El Ghadioui R., 2020. Bemessung carbonbewehrter Betonbauteile unter besonderer Betrachtung des Gebrauchszustandes: Entwicklung eines Modells zur wirklichkeitsnahen Verformungsberechnung [PhD dissertation], 1st ed., Technische Universität Darmstadt, Institut für Massivbau, Darmstadt.